Chapter 14

A Localization System for Mobile Robot Using Scanning Laser and Ultrasonic Measurement

14.1. Introduction

The ability of locating itself in the environment is essential for a mobile robot to execute its commands. Localization is fundamental to subsequent tasks such as map building and collision-free path planning. Various methods have been developed by many researchers. A review on the mobile robot localization technologies can be found in [BOR 97]. Among those, odometry was widely used to determine the momentary position. Borenstein and Feng [BOR 96] improved the accuracy of odometry up to one order of magnitude by measuring and correcting the robot's systematic errors. However, wheel slippage and ground roughness would cause a fatal error in the robot's heading measurement, which could later introduce a significant position error, should the robot travel a long way. In order to improve the robot's heading accuracy as well as the dead reckoning accuracy, gyroscope was used and tested by many researchers [KOM 94, HAR 96, FEN 96, BOR 98, CHU 01]. The dead reckoning method using a gyroscope can avoid the influence of wheel slippage and ground roughness on a robot heading measurement, and hence provides a more accurate momentary position and heading than odometry does. But low-cost gyroscopes suffers from random

---

Chapter written by Kai LIU, Hongbo LI and Zengqi SUN.

drift over long-time running. Dead reckoning is a relative localization method, and may suffer from unbounded accumulative errors. To compensate this, an absolute method must be used. Triangulation using landmarks is a commonly adopted method [COH 92, BET 97, FON 05]. To use artificial landmark triangulation, the position of each landmark must be known. This is not convenient when the robot's working environment is unstructured. To use natural landmark triangulation, an accurate map for the environment should be available. Often, to build a map of the robot's environment is a tough task for users. Tsai [TSA 98] combined a flux gate compass, a rate-gyro and two encoders to get an optimal estimate for robot heading, and combined the dead reckoning position estimate with ultrasonic range measurements to remove accumulated position errors, but the coverage of the ultrasonic transmitter was limited to a small area. And this method fails in the environment where the magnetic field of the earth is twisted. Vision-based localization and simultaneous localization and mapping (SLAM) are regarded as key essentials for a real autonomous mobile robot and have been widely researched in recent years [SE 05, ROY 07]. But the computational complexity hinders their realistic application.

Our efforts focus on developing a simple, low-cost, continuously accurate and convenient method of mobile robot localization using a multisensor. We assume that the mobile robot has a base station fixed to the ground where the robot can recharge itself. The robot's position and heading are relative to the base station. The method's novelty lies in the combination of scanning laser and ultrasonic measurement to construct an absolute localization system. A scanning laser and an ultrasonic transmitter are mounted on the base station to measure the robot's angle and distance relative to it. Another scanning laser is mounted on the robot to measure the base station's relative angle in the robot's frame. The base station and the robot are wirelessly connected through radio frequency (RF). Using the extended Kalman filter, the data of a scanning laser and ultrasonic absolute positioning system are fused with the dead reckoning system that utilizes a low-cost gyroscope. This method achieves the convenience that neither an extra artificial landmark nor an accurate map of the environment is needed, and it is suitable for both a structured and an unstructured environment.

The chapter is organized as follows. Section 14.2 describes the mechanical and electronic hardware configuration of our positioning system. Section 14.3 details the proposed method. The performance of the method is given in section 14.4. Section 14.5 presents our conclusion.

14.2. System configuration

The mechanical structure of our mobile robot is typical, which consists of two independently driven back wheels and a freely rotating front wheel. The robot has a digital signal processing (DSP) unit as its central controller. A low-cost and high drifting numerical Micro-Electro-Mechanical Systems (MEMS) gyroscope ADIS16255 is utilized in dead reckoning. Two optical incremental encoders are mounted on the driving motors to provide the odometry information of each wheel for the dead reckoning. A compass is not used for the reason that in some environments the magnetic field is twisted and it will lose its function or bring error heading information to the robot, especially when the magnetic field's direction changes slowly from place to place.

Because of the wheel slippage, surface roughness and gyro-drift, there is accumulative error in the robot position estimation. So, an absolute positioning system is needed to compensate the accumulative error in the dead reckoning system. To improve the convenience of installation, we make full use of the base station and no extra landmark is needed. According to polar coordinates system, to locate the robot, the angle and distance of the robot in the base station polar coordinates system should be known. A laser scanner with a high-resolution optical encoder is mounted on the base station to get the polar angle. An ultrasonic wave transmitter is attached to the scanning laser and rotates with it. Figure 14.1 shows the structure.

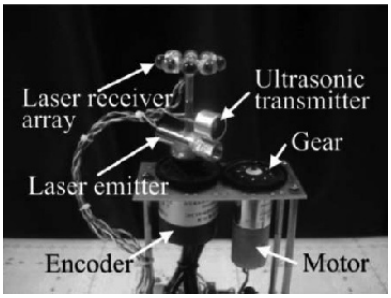

Figure 14.1. *Assembling structure of the scanning laser, ultrasonic transmitter and the laser receiver array on base station*

A laser receiver array and an ultrasonic wave receiver array are mounted on the robot. They can receive the laser and ultrasonic wave that comes from any direction from the base station. Figure 14.2 shows the structure.

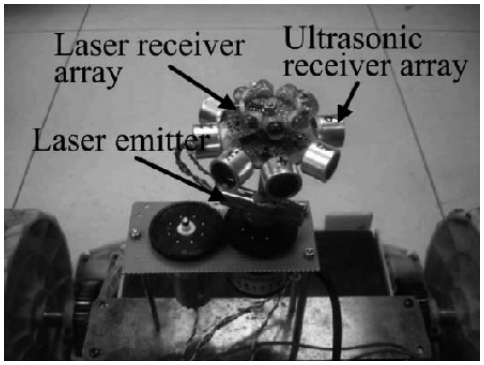

Figure 14.2. *Assembling structure of the laser receiver array, ultrasonic receiver array and the laser emitter on robot*

When the laser is received by the robot, it sends an RF signal to the base station to indicate that the robot is scanned by the base. Then, the base station sends the angle of the scanning laser encoder to the robot and emits an ultrasonic wave pulse after that. Since the time delay from the RF transmitting to the ultrasonic wave sending is constant, the time of flight (TOF) of the ultrasonic wave can be measured so as to obtain the distance from the base station to the robot.

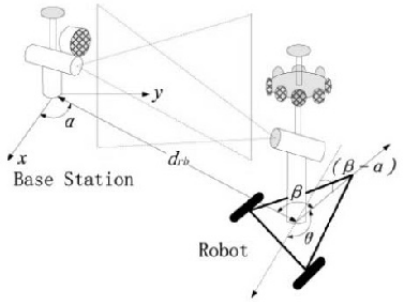

Figure 14.3. *Sketch of the scanning laser and ultrasonic absolute positioning system*

To compensate the angle drift of the low-cost gyroscope, we mounted another scanning laser on the robot, and the laser's direction is also measured by a high-resolution optical incremental encoder, as shown in Figure 14.2. The laser line emitted by the base station and the robot are modulated to

different frequencies to avoid mutual and sunlight interruption. The base station also has a laser receiver array to receive the laser from the robot. When the robot laser is received by the base station, it sends an RF signal to the robot. The moment robot receives the signal from the base station, the angle of the scanning laser encoder is read out. Together with the position of the base station and the robot, the robot heading can be calculated. And then fused with the gyroscope information, the optimal robot heading is estimated.

A sketch of the scanning laser and ultrasonic absolute positioning system is shown in Figure 14.3.

14.3. Implementation

14.3.1. *Dead reckoning system*

When the robot is not scanned by the base station, it works in a dead reckoning mode. Tsai [TSA 98] used a multisensorial scheme fusing data from a gyro, a flux compass and two encoders to get an optimal estimate of the robot heading. But when we apply this method, it fails when the direction of the Earth's magnetic field changes slowly from place to place. In this condition, the absolute difference between the compass heading and gyro heading is less than the selected threshold in every sampling period (0.5 s), and the error information in a compass is fused in the robot heading. Gradually, the robot heading converges to the direction of the magnetic field, which has been twisted. This is because the error model in a compass measurement is not a discrete-time, zero-mean white Gaussian process when the magnetic field is slowly twisted. So in our system, we measure the robot relative heading by fusing information from a gyro and two encoders, and later fuse the relative heading with scanning laser angle information when the base station is scanned by the robot. Let $\theta_e(k)$ and $\theta_e(k-1)$ denote the robot heading angle estimated by using the information from two wheel encoders at time k and $(k-1)$, so $\theta_e(k)$ can be calculated by:

$$\theta_e(k) = \theta_e(k-1) + (\Delta p_r c_r - \Delta p_l c_l) / d + n_e(k) \qquad [14.1]$$

where Δp_r and Δp_l denote the pulse increase of right encoder and left encoder from time $(k-1)$ to time k. d denotes the distance between the driven wheels. c_r and c_l convert the encoder pulse to distance traveled by the right and left wheels in millimeters. In order to get the accurate value of c_r and c_l, we manually drive the robot to track along a straight line path for a

distance l, and read the pulse increase p_r and p_l. The c_r and c_l can be calculated by $c_r = l/p_r$ and $c_r = l/p_l$. Several measurements are needed to increase accuracy by calculating the average value of c_r and c_l. Measurement noise $n_e(k)$ is assumed to be a zero-mean white Gaussian process with variance σ_e^2.

Let $\theta_g(k)$ and $\theta_g(k-1)$ denote the robot heading angle estimated from a gyroscope. For convenience, we rewrite here the equation of the gyro heading measurement in [TSA 98]:

$$\theta_g(k) = \theta_g(k-1) + \int_{(k-1)T}^{kT} \dot{\theta}(t)dt + n_g(k) \qquad [14.2]$$

where $\theta(t)$ is the gyro's rotational rate. T is the integration period. The noise $n_g(k)$ is also assumed to be a zero-mean white Gaussian process with variance σ_g^2. According to [TSA 98], if the absolute difference between $\theta_e(k)$ and $\theta_g(k)$ is less than a selected threshold, the dead reckoning optimal robot heading estimated by fusing information from the gyro and two encoders is:

$$\theta_d(k) = \frac{\theta_e(k)\sigma_g^2 + \theta_g(k)\sigma_e^2}{\sigma_g^2 + \sigma_e^2} \qquad [14.3]$$

otherwise, $\theta_d(k) = \theta_g(k)$. After the fusing, we let $\theta_e(k) = \theta_g(k) = \theta_d(k)$.

The gyro and encoder information updating period that we use is 10 ms to provide the robot real-time heading information that is needed in its real-time control. $\theta_e(k)$ and $\theta_g(k)$ are fused every 0.5 s. We call it the fusing period. In between the fusing period, $\theta_d(k)$ is equal to $\theta_g(k)$. If the fusing period is too small, the error between $\theta_e(k)$ and $\theta_g(k)$ will be constantly below the threshold even when wheel slippage occurs. Therefore, error information will be fused in the robot heading.

Next, the robot's dead reckoned position (x_d, y_d) is updated every 10 ms by:

$$x_d(k) = x_d(k-1) + \Delta x_d \qquad [14.4]$$

$$y_d(k) = y_d(k-1) + \Delta y_d \quad [14.5]$$

where

$$\Delta x_d = \frac{\Delta p_r c_r + \Delta p_l c_l}{2} \cos\left(\frac{\theta_d(k) + \theta_d(k-1)}{2}\right) \quad [14.6]$$

$$\Delta y_d = \frac{\Delta p_r c_r + \Delta p_l c_l}{2} \sin\left(\frac{\theta_d(k) + \theta_d(k-1)}{2}\right) \quad [14.7]$$

14.3.2. *Scanning laser and ultrasonic positioning system*

The dead reckoning positioning system is relative and will suffer from unbounded accumulative error. Therefore, an absolute positioning system is needed to eliminate the accumulative error in the robot heading and position in time. The scanning laser mounted on the base station scans the robot repeatedly. When the robot is scanned by the base station, it sends an RF signal. When the base station receives the RF signal, it sends the scanning laser angle α (shown in Figure 14.3) to the robot also through RF and then emits an ultrasonic wave pulse immediately. Let t_{rf} denote the moment when the RF (which contains the scanning laser angle) is received by the robot, and t_{ul} denote the moment when ultrasonic wave pulse is received by the robot. The radio signal travels in the air at light speed. So its flying time can be ignored, then the ultrasonic flying time is:

$$t_f = t_{ul} - t_{rf} - t_0 \quad [14.8]$$

where t_0 denotes the system's constant time delay from the RF transmitting to the ultrasonic wave sending in the base station and the RF receiving delay in the robot. As the sound speed is related to the density of air, there is a temperature sensor on the robot to compensate the sound speed variance. So, the distance between the robot and the base station, d_{rb}, is measured. Along with the angle of the scanning laser, the robot's absolute position (x_a, y_a) in the frame of base station can be calculated by:

$$x_a = d_{rb} \cos(\alpha) \quad [14.9]$$

$$y_a = d_{rb} \sin(\alpha) \quad [14.10]$$

If the distance between the dead reckoned position and the absolute position measured by a scanning laser and a ultrasonic positioning system is less than a selected threshold, the absolution position (x_a, y_a) is fused with the

dead reckoning system by extended Kalman filter. We define $X(k) = (x(k), y(k))$, $X_d(k) = (x_d(k), y_d(k))$ and let $K(k)$ denote the Kalman filter error gain at time k. The extended Kalman filter consists of the following steps:

1) The one-step optimal prediction $\hat{X}(k|k-1)$ should be the dead reckoned position $X_d(k)$ calculated by equations [14.4], [14.5], [14.6] and [14.7]. Thus,

$$\hat{X}(k \mid k-1) = X_d(k) \qquad [14.11]$$

Its propagation error covariance matrix $\tilde{P}(k \mid k-1)$ can be calculated by:

$$\tilde{P}(k \mid k-1) = \tilde{P}(k-1 \mid k-1) + Q(k-1) \qquad [14.12]$$

where $\tilde{P}(k-1 \mid k-1)$ is the error covariance matrix of optimal estimate $\hat{X}(k-1 \mid k-1)$ at time $k-1$, and $Q(k-1)$ is the diagonal covariance matrix of process noises.

2) Since the robot's position state $X(k)$ can be returned by the scanning laser and ultrasonic positioning system, the state transition matrix $F(k+1, k)$ and observation matrix $C(k)$ should be a unit matrix, so $K(k)$ is calculated by:

$$K(k) = \tilde{P}(k \mid k-1)[\tilde{P}(k \mid k-1) + R(k)] \qquad [14.13]$$

where $R(k)$ denotes the diagonal covariance matrix of measurement noises.

3) Then, we can get the robot position's optimal estimate $\hat{X}(k|k)$ and update the error covariance matrix $\tilde{P}(k \mid k)$ using:

$$\hat{X}(k \mid k) = \hat{X}(k \mid k-1) + K(k)[X_a(k) - \hat{X}(k \mid k-1)] \qquad [14.14]$$

$$\tilde{P}(k \mid k) = [I - K(k)]\tilde{P}(k \mid k-1) \qquad [14.15]$$

where $X_a(k)$ denotes the robot absolute position calculated by [14.9] and [14.10] at time k, namely $X_a(k) = (x_a(k), y_a(k))$. After the fusing, we let

$$(x_d(k), y_d(k)) = (x(k), y(k)) \qquad [14.16]$$

to eliminate the accumulative error in dead reckoned position.

There is also a scanning laser with a high-resolution encoder mounted on the robot in order to compensate for the accumulative error in robot orientation. The moment the base station is scanned by the robot, it also sends a signal to the robot through RF. The robot then receives the signal and records the robot scanning laser angle β in the robot frame (shown in Figure 14.3). Let α denote the angle the robot's position is at in the base station frame. Therefore,

$$\alpha = \arctan(y(k) / x(k)) \qquad [14.17]$$

where $(x(k), y(k))$ is the optimal estimate of the robot's position at time k. So, the robot's heading from the scanning laser can be calculated by:

$$\theta_l(k) = \pi - (\beta(k) - \alpha(k)) + n_l(k) \qquad [14.18]$$

where $n_l(k)$ is the measurement noise, which is also assumed to be a zero-mean white Gaussian process with variance σ_l^2. Figure 14.3 shows the relationship of θ, β and α in [14.18]. Also, if the absolute error between θ_l and θ_d is less than a selected threshold, for example 3°, the robot's optimal heading can be estimated by:

$$\theta(k) = \frac{\theta_d(k)\sigma_l^2 + \theta_l(k)\sigma_d^2}{\sigma_l^2 + \sigma_a^2}. \qquad [14.19]$$

where the dead reckoned robot heading $\theta_d(k)$ is also assumed to be a zero-mean white Gaussian process with variance σ_d^2 After the estimation, we let $\theta_d(k) = \theta$ to eliminate the accumulative error in dead reckoning angle.

Furthermore, with the scanning laser and the ultrasonic absolute positioning system, the robot can initialize its position and heading at any position and orientation within the system's effective range. To do this, the robot first calculates its initial position through [14.9] and [14.10], and then the heading can be calculated by [14.17] and [14.18].

14.4. Experimental results

We applied the proposed localization system to a lawn robot as shown in Figure 14.4 and our objective is to make it work for a long period of time (e.g. for about one hour) without losing its position, where the lawn robot is designed to mow the lawn with coverage planning rather than randomly.

Therefore, it would not surpass the lawn edge during its mowing work without the assistance of a buried electric wire, which is needed by such current products. In our experiments, the base station is placed at origin (0,0). The scanning laser on the base station and the robot slowly scans from side to side with a period of 5 s.

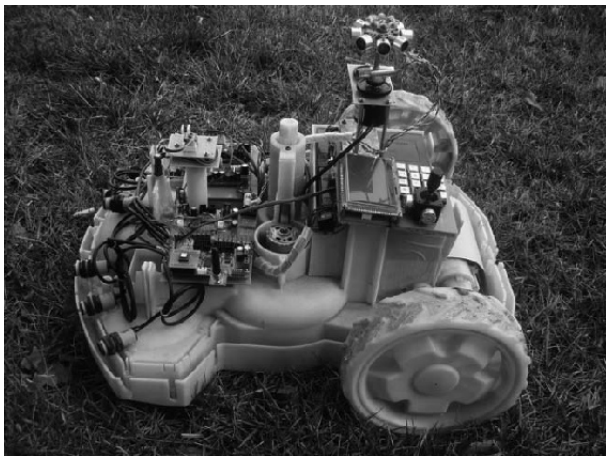

Figure 14.4. *The experimental lawn robot*

We first conduct an experiment to evaluate the accuracy of the ultrasonic distance measurement on which the performance of the scanning laser and ultrasonic absolute localization system largely depends. The lawn robot is placed at four different distances away from the base station: 240, 1,200, 2,100 and 3,000 cm. When the distance is larger than 35 m, the ultrasonic wave becomes so weak that the receiver array on the robot fails to receive it. Figure 14.5 shows the accuracy. There are 40 measurements at each distance. The respective mean square errors of the four curves in Figure 14.5 are 2.9, 3.0, 5.4 and 8.3 cm. The absolute errors stay well within 10 cm when the distance is approximately 10 m and less. The error becomes larger when the robot gets farther, but stays mostly within 10 cm when the distance is about 20 m. Even at the range of 30 m, the measurement error is acceptable at the 10 cm order of magnitude. The occasional wrong measurements with the absolute error lager than 15 cm can be filtered out by the data fusing strategy.

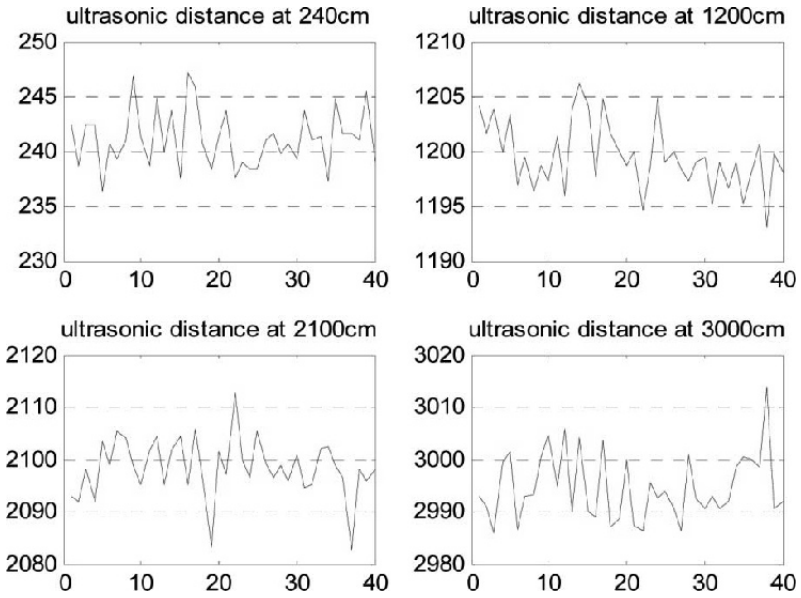

Figure 14.5. *Accuracy of scanning laser and ultrasonic positioning system*

The next experiment aims at evaluating the accuracy of the scanning laser and ultrasonic absolute positioning system. The robot stops at several specified points in the environment and its position is calculated using the information coming from the scanning laser and the ultrasonic distance measurement. Figure 14.6 shows the results. The crossing point of the dashed line in each subfigure is the robot's specified position, and the circles denote its calculated position by the absolute positioning system, namely (x_a, y_a). The calculated position in each subfigure seems to be classified into two clusters. This is due to the angle error of the base station scanning laser. Our encoder linked with the scanning laser has a resolution of 1,000 pulses per circle. Therefore, one pulse error in the pulse counter will lead to 0.36° error in the angle measurement. Using encoders of higher resolution will have higher accuracy. The position error led by the angle becomes larger when the robot gets farther away from the base station. Within each point cluster, the error is caused by the fluctuation in ultrasonic distance measurement. As we can see from Figure 14.6, this scanning laser and ultrasonic positioning system is effective when the robot works within 30 m from the base station with the position error being kept at a 10 cm order of magnitude.

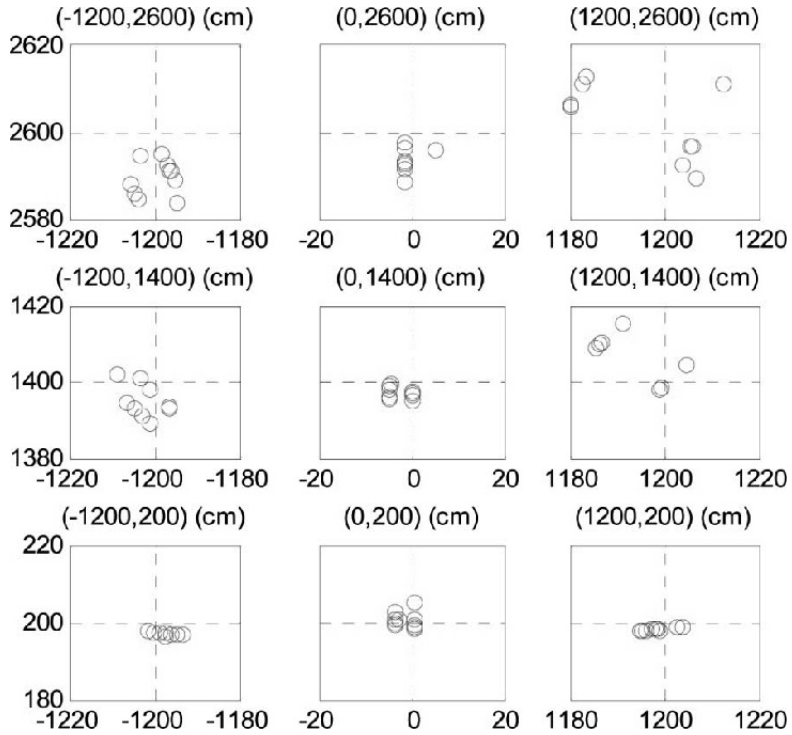

Figure 14.6. *Accuracy of ultrasonic distance measurement (cm)*

The last experiment evaluates the robot's real-time running performance with the dead reckoning fused with the scanning laser and ultrasonic positioning system. Before the experiment, the parameters of noise models are calculated, where $\sigma_g^2 = 2$, $\sigma_e^2 = 2$, $\sigma_d^2 = 2$, $\sigma_l^2 = 2$, $Q(k) = Q(k-1) = diag\{1000, 1000\}$ and $R(k) = R(k-1) = diag\{1000, 1000\}$. The initial conditions of Kalman filter are $\hat{X}(0|0) = (0, 1200)$ and $\tilde{P}(0|0) = diag\{1000, 1000\}$ (angle unit: degree, distance unit: mm). The experiment was performed on an outdoor lawn. We first manually drive the robot carefully along a 24 m × 24 m square shape path marked on the lawn by white tape. (The white tape is only used to assist the driver in steering the robot exactly on the desired path, and not used for robot navigation.) In the progress, the robot's calculated position is stored in its memory for every 60 cm traveled.

Then, the stored data are sent to the computer through serial port. Figure 14.7 shows that the calculated position fits well with robot trajectory.

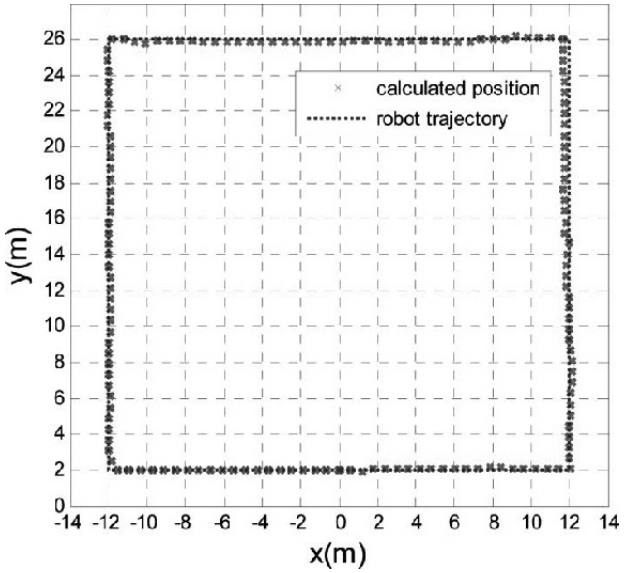

Figure 14.7. *Robot trajectory and its calculated position*

After that, we let the robot navigate itself automatically along the 24 m × 24 m square path, as shown by the dotted path in Figure 14.7, which was also preprogrammed in the robot. Since it is difficult to measure the robot's position error during its navigation, we measure its position when it returns and stops at the starting point (0, 200 cm). This error measuring method was used in [BOR 96] and [CHU 01]. But during our measurement, the robot's software program remains running, and it keeps navigating after the measurement is done. This is in an effort to test the robot's continuous localization ability for long-time running. There are 20 continuous runs with each run lasting about 2.5 min. Both clockwise and anticlockwise measurements are tested. Let (x_r, y_r) denote the tape measured point where the robot returns and (x_c, y_c) denote its calculated position. The error points $(x_r - x_c, y_r - y_c)$ between the returning points and the calculated position are denoted by small squares (clockwise measurements) and circles (anticlockwise measurements) in Figure 14.8. Although the position error becomes reasonably larger when the robot gets farther, the returning point

error at (0, 200 cm) keeps robustly within a 10 cm order of magnitude. The accumulative error of relative dead reckoning is effectively compensated by fusing with the absolute positioning system. This confirms that the proposed method is convergent over long-time running.

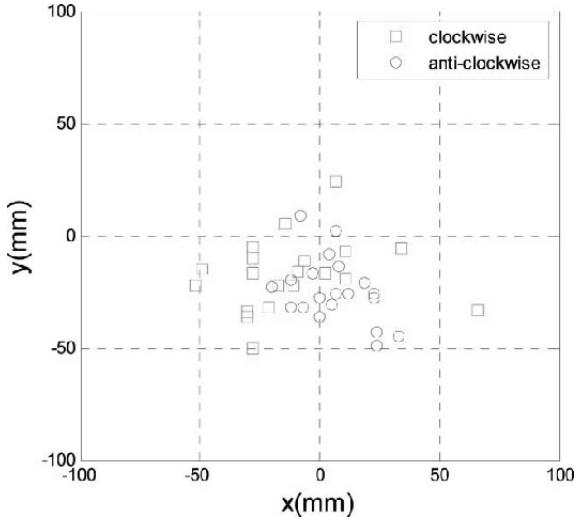

Figure 14.8. *Robot trajectory and its calculated position*

14.5. Conclusion

This chapter has developed a low-cost, simple and convenient multisensor-based mobile robot localization system. The information from a low-cost gyro and two wheel encoders are fused to get the robot's temporary heading and position. A scanning laser angle measurement and ultrasonic distance measurement system is employed to eliminate the accumulative error in robot's dead reckoned heading and position. The proposed localization system can work both indoors and outdoors and needs no artificial landmarks or accurate map of the robot's working environment, only a base station is needed. Experimental results show that the system works well on a lawn robot. With our localization system, the lawn robot can work on the lawn continuously for a long period of time within 30 m from the base station. The lawn edge can be stored in the robot to avoid it surpassing the edge. Furthermore, the robot can initialize itself at any position within the system's effective range.

14.6. Acknowledgments

This work was supported by the Yangtze Delta Region Institute of Tsinghua University, Zhejiang, China. The first author of this chapter is sincerely appreciative of their kind cooperation. This work was also supported in part by the National Basic Research Program of China (973 Program) under Grant 2012CB821206, by the National Natural Science Foundation of China under Grants 61004021, 61174069 and 61174103, and by the Beijing Natural Science Foundation under Grant 4122037.

14.7. Bibliography

[BET 97] BETKE M., GURVITS L., "Mobile robot localization using landmarks", *IEEE Transactions on Robotics and Automation*, vol. 13, no. 2, pp. 251–263, 1997.

[BOR 96] BORENSTEIN J., FENG L., "Measurement and correction of systematic odometry errors in mobile robot", *IEEE Transactions on Robotics and Automation*, vol. 12, no. 6, pp. 869–880, 1996.

[BOR 97] BORENSTEIN J., EVERETT H.R., FENG L., "Mobile robot positioning – sensors and techniques", *Journal of Robotic Systems*, vol. 14, no. 4, pp. 231–249, 1997.

[BOR 98] BORENSTEIN J., "Experimental evaluation of a fiber optics gyroscope for improving dead-reckoning accuracy in mobile robots", *IEEE International Conference on Robotics and Automation*, Leuven, Belgium, pp. 3456–3461, 16–20 May 1998.

[CHU 01] CHUNG H., OJEDA L., BORENSTEIN J., "Accurate mobile robot dead-reckoning with a precision-calibrated fiber optic gyroscope", *IEEE Transactions on Robotics and Automation*, vol. 17, no. 1, pp. 80–84, 2001.

[COH 92] COHEN C., KOSS F.V., "A comprehensive study of three object triangulation", *SPIE Conference on Mobile Robots*, Boston, MA, USA, pp. 95–106, 18–20 November 1992.

[FEN 96] FENG L., BORENSTEIN J., "Gyrodometry: a new method for combining data from gyros and odometry in mobile robots", *IEEE International Conference on Robotics and Automation*, Minneapolis, MN, pp. 423–428, 22–28 April 1996.

[FON 05] FONT J.M., BATLLE J.A., "Dynamic triangulation for mobile robot localization using an angular state kalman filter", *European Conference on Mobile Robots*, Ancona, Italy, pp. 20–25, 7–10 September 2005.

[HAB 07] HABIB M.K., "Real time mapping and dynamic navigation for mobile robots", *International Journal of Advanced Robotic Systems*, vol. 4, no. 3, pp. 323–338, 2007.

[HAR 96] HARDT H.J., WOLF D., HUSSON R., "The dead reckoning localization system of the wheeled mobile robot ROMANE", *IEEE/SICE/RSJ International Conference on Multisensor Fusion and Integration for Intelligent Systems*, Washington, DC, pp. 603–610, 8–11 December 1996.

[KOM 94] KOMORIYA K., OYAMA E., "Position estimation of a mobile robot using Optical Fiber Gyroscope (OFG)", *International Conference on Intelligent Robot and System (IROS '94)*, Munich, Germany, pp. 143–149, 12–16 September 1994.

[ROY 07] ROYER E., LHUILLIER M., DHOME M., "Monocular vision for mobile robot localization and autonomous navigation", *Internal Journal of Computer Vision*, vol. 74, no. 3, pp. 237–260, 2007.

[SE 05] SE S., LOWE D.G., LITTLE J.J., "Vision-Based global localization and mapping for mobile robots", *IEEE Transactions on Robotics*, vol. 21, no. 3, pp. 364–375, 2005.

[SUZ 92] SUZUKI S., HABIB M.K., YUTA, S., *et al*., "How to describe the mobile robot's sensor based behavior", *The Journal of Robotics and Autonomous Systems*, vol. 7, nos. 2–3, pp. 227–237, 1992.

[TSA 98] TSAI C.C., "A localization system of a mobile obot by fusing dead-reckoning and ultrasonic measurements", *IEEE Transactions on Instrumentation and Measurement*, vol. 47, no. 5, pp. 1993–1998, 1998.